Supporting Information

High Performance As-Cast Non-Fullerene Polymer Solar Cells from Benzo[1,2-b:4,5-b']difuran Polymer via Rational Copolymer Design

Enfang He [a], Zhi Zheng,[a] Yi Lu, [a] Fengyun Guo, [a] Shiyong Gao, [a] Genene Tessema Mola, [c] Liancheng Zhao, [a] Yong Zhang* [a,b]

[a]School of Materials Science and Engineering, Harbin Institute of Technology, Harbin 150001, China

E-mail: yongzhang@hit.edu.cn

[b]School of Materials Science and Engineering, Zhengzhou University, Zhengzhou 450001, China

[c]School of Chemistry and Physics, University of KwaZulu-Natal, Pietermaritzburg Campus, Scottsville 3209, South Africa

1. Experimental Section

Materials: All chemicals and solvents were purchased from commercials and used directly without further purification except mention. TBz-Br and (4,8-bis(4-(2-butyloctyl)-3,5-difluoro phenyl)benzo[1,2-b:4,5-b']difuran-2,6-diyl) bis (trimethyl stannane) (DiFPBDF-Tin) and TCO2-Br were synthesized according to the procedure reported in the literatures.[1-3] The electron acceptor IT-4F was purchased from Derthon Optoelectronic Materials Science Technology Co LTD.

Synthesis of BDF-based polymer F13-R

The 0.2 mmol DiFPBDF-Tin monomer and 0.2 mmol blend monomer of TBz-Br and TCO2-Br (0.16 mmol TBz-Br/0.04 mmol TCO2-Br) were dissolved in 5 mL of toluene, and then the solution was purged with argon for 5 min. The catalyst, $Pd(PPh_3)_4$ (5 mg), was added in one portion, and the mixture was purged with argon for another 20 min. The reaction was then stirred at 110 °C for 6 h under argon protection. The polymer solution was cooled to room temperature and precipitated from 50 mL of methanol then collected by filtration and then subjected to Soxhlet extraction with methanol, hexane, and chloroform in the end. The polymers were recovered as solid from the chloroform fraction by precipitation from methanol, and collected as metallic purple solid with a yield of around 60% after dry in vacuum.

The weight-average molecular weight of F13-R is 30.2 kDa, which was similar to that of F13-R with weight-average molecular weight of 29.5 kDa.

2. Material Characterizations

UV-visible absorption spectra were measured via Beijing Purkinje General-TU-1901 spectrophotometer. Cyclic voltammetry was performed on a CH Instruments CHI660E electrochemical workstation with a three-electrode system in 0.1 M $[Bu_4N]PF_6$ acetonitrile solution at a scan rate of 40 mV/s. ITO with sample film was used as the working electrode. A Pt wire was used as the counter electrode and Ag/AgCl was used as the reference electrode.

Ferrocene/ferrocenium redox couple was used as the external standard and its redox potential is 0.45 V vs. Ag/AgCl. The HOMO and LUMO energy levels were calculated from the onset of the oxidation and reduction potentials. Atomic force microscopy (AFM) images were obtained using a NanoMan VS microscope in the tapping mode. The interaction parameter χ is defined as $\chi = K(\sqrt{\gamma_{donor}} - \sqrt{\gamma_{acceptor}})^2$, where K is a constant (K=1), γ_{donor} is the surface tension of F13 or F13-R donor, $\gamma_{acceptor}$is the surface tension of IT-4F acceptor. Surface energies could be resolved into nonpolar (dispersion) and polar components, which can be calculated based on contact angles obtained by the water and glycerol

3. Device Fabrication and Characterization

These PSCs devices were fabricated with the inverted structure of ITO/ZnO/active layer/MoO_3/Ag in a N_2-filled glovebox and characterized in the air without encapsulation. The ITO-coated glass substrates were cleaned with isopropyl alcohol, dishwashing liquid, deionized water, ethanol, acetone, and isopropanol for 30 min, respectively. The ZnO precursor (concentration of solution: 0.45 M) was prepared by dissolving zinc acetate [$Zn(CH_3COO)_2 \cdot 2H_2O$] in 2-methoxyethanol containing ethanolamine as a stabilizer. After ITO being dried, the ZnO precursor was spin-coated onto the cleaned ITO glass at 4000 rpm/min for 30s and annealed in the titanium plate under 250 ^{o}C for 30 mins. The active layer was spin-coated in a N_2-filled glovebox from a solution of Polymer:IT-4F with 1:1.5 weight ratio in chlorobenzene without additives and thermal annealing or solvent vapor annealing except the optimization process. Finally, 1 nm MoO_3 and 100 nm Ag were sequentially evaporated on the active layer in the vacuum chamber under a pressure of ca. 2.5×10^{-4} Pa. The effective area of one cell is 4 mm^2. The current-voltage (J-V) characteristics of the devices were measured on a Keithley 2450 Source Measure Unit. The power conversion efficiency (PCE) was measured under an illumination of AM 1.5G (100 mW/cm^2) using a SS-F5-3A (Enli Technology Co. Ltd.) solar simulator (AAA grade, 50 mm x 50 mm photobeam size). The EQE was measured by Solar Cell Spectral Response Measurement System QE-R3011 (Enli Technololy Co. Ltd.). The light intensity at each wavelength was calibrated with a standard single-crystal Si photovoltaic cell.

Hole-only device with the structure of ITO/PEDOT:PSS/ Polymer:IT-4F/MoO_3/Ag and the electron-only device with the structure of ITO/ZnO/ Polymer:IT-4F/Ca/Al were fabricated. PEDOT:PSS (Heraeus Clevios P VP A 4083) was spin-cast from aqueous solution at 3000 rpm for 30 s (40 nm), then dried at 150 °C for 15 min in air. 20 nm Ca and 100 nm Al were sequentially evaporated in the vacuum chamber under a pressure of ca. 2.5×10^{-4} Pa. The mobility was determined by fitting the dark current to the model of a single carrier SCLC, which is described by the equation:

$$J = \frac{9}{8} \varepsilon_0 \varepsilon_r \mu_h \frac{V^2}{d^3}$$

Where J is the current, μ_h is the zero-field mobility,ε_0 is the permittivity of free soace, ε_r is the relative permittivity of the material, d is the thickness of the active layer, and V is the effective voltage.

4. Figures and Tables

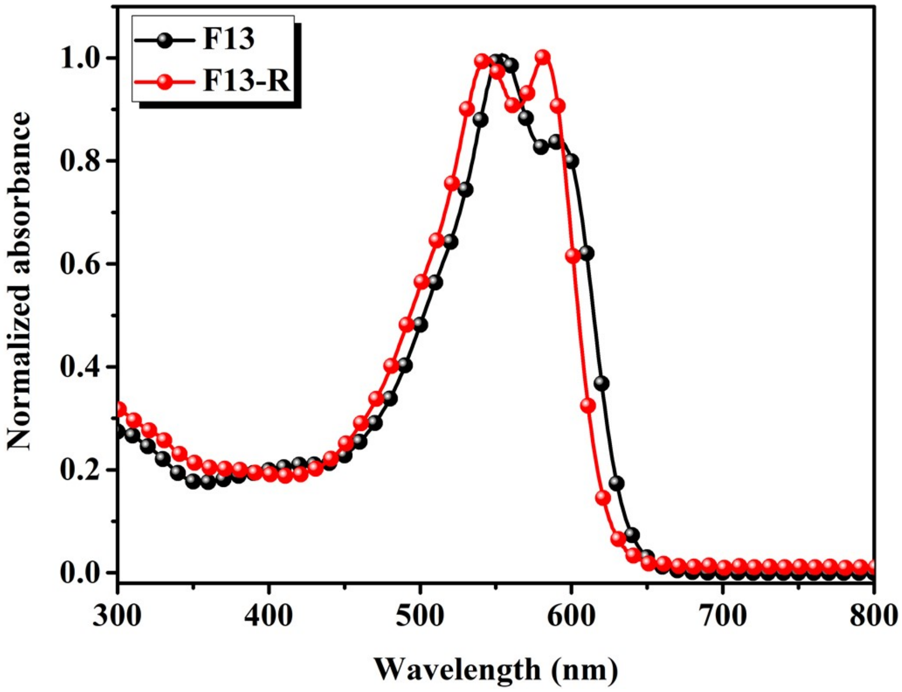

Fig. S1. Normalized UV-vis absorption spectra of F13-R and F13 in chlorobenzene solution

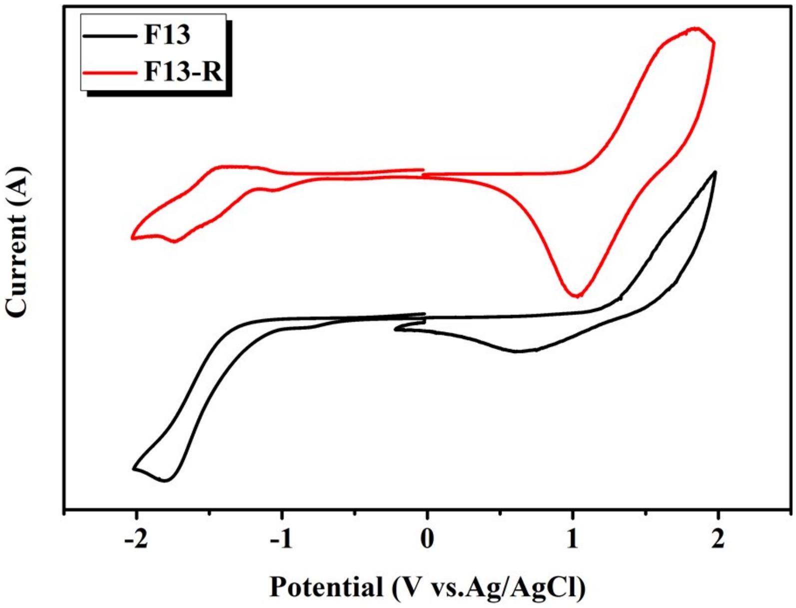

Fig. S2. Cyclic voltammograms of the F13 and F13-R films on glassy carbon electrodes in 0.1 mol L^{-1} Bu_4NPF_6 of acetonitrile solution at a scan rate of 40 mV/s

Table S1. The average parameters of 20 independent as-cast F13-R:IT-4F devices.

D:A	V_{oc}[V]	Jsc[mA/cm^2]	FF(%)	PCE[%]
F13-R:IT-4F	0.892±0.008	17.52±0.14	76.10±0.90	11.9±0.2

Table S2. The summary of V_{oc}, Jsc, FF, PCE and of as-cast binary PSCs from single solvent without solvent additive as well as thermal or solvent annealing treatment.

D:A	V_{oc}[V]	Jsc[mA/cm^2]	FF(%)	PCE[%]	Reference
PDBT-T1:IC-C6IDT-IC	0.89	15.05	65	8.71%	4
PBDT-DFQX-TTSC8:$PC_{71}BM$	0.85	14.63	68.23	8.51%	5
PBDT-DFQX-TSEH:$PC_{71}BM$	0.85	12.58	66.12	7.02%	
PM6:IDIC	0.97	17.8	69	11.90%	6
DI3T:$PC_{71}BM$	0.85	3.63	27	0.83%	7
DI3T-2F:$PC_{71}BM$	0.84	13.0	71.8	7.80%	
PBDB-T:4TIC-4F	0.65	21.5	57	7.99%	8
PBDB-T:6TIC-4F	0.72	23.0	67	11.14%	
TB7-Th:ITVfIC	0.74	17.54	63.11	8.21%	9
PBDB-T:IDTCN-C	0.84	20.33	69.6	11.92%	10
PBDB-T:IDTCN-O	0.91	19.96	73.2	13.28%	
PBDB-T:IDTCN-S	0.85	19.04	65.7	10.60%	
PBDB-T:IDTT2F	0.81	18.51	59	8.85%	
PBDB-T:m-INPOIC	0.85	20.7	66.9	12.10%	11
PBDB-T:p-INPOIC	0.85	18.4	66.1	10.60%	
PBDB-T:INPIC-4F	0.84	17.9	63.2	9.71%	
PFBDB-T:CDTTIC	0.78	25.8	57	11.50%	12
PTB7-Th:FOIC	0.74	24.0	67.1	12.00%	13
PTB7-Th: ITIC3	0.76	16.8	63.1	8.09%	
PBDB-T:PDT-T	0.88	18.88	66.3	11.02%	14
PBDB-T:PDT	0.97	13.48	54	7.07%	
P2F-EHp:BTPTT-4F(Y6)	0.90	22.69	54.68	11.14%	15
PBDB-T-SF:IDIC	0.98	15.29	62.65	9.39%	16
PBDB-T-SF:ID4F	0.82	17.42	72.47	10.35%	
PBFTT:IT-4Cl	0.76	19.7	73.9	11.10%	17
PBDB-T:PSM1	0.95	9.08	55.59	5.17%	18

PBDB-T:PSM2	0.91	9.08	46.07	3.81%	
PBDB-T:PSM3	0.99	12.51	54.00	6.71%	
DI3T-1F:$PC_{71}BM$	0.82	13.6	75.1	8.33%	19
DI3T-2F:$PC_{71}BM$	0.84	12.8	68.5	7.32%	
PM7:C8-IT-4F	0.82	22.7	77.1	14.3%	20
PBOTT:IT-4Cl	0.84	14.95	65.5	8.25%	21
PBOTVT:IT-4Cl	0.66	8.87	53.1	3.12%	
PBOffDT:IT-4Cl	0.86	18.27	67.1	10.56%	
D18:Y6Se	0.839	27.98	75.3	17.7%	22
PBDB-T:COTh-FPDI	0.98	12.68	67.52	8.37%	23
PBDB-T:COTh-αPDI	0.86	10.89	58.95	5.51%	
PBDB-T:COTh-PDI	0.88	11.45	55.57	5.58%	
P3HT:PCBM	0.58	10.1	64.8	3.80%	24
PM6:DCB-4F	1.00	16.42	58.23	9.56%	25
PM6:CB-4F	0.86	2.84	31.97	0.78%	
F13:IT-4F	0.82	9.11	53.86	4.02%	This work
F13-R:IT-4F	0.904	17.61	76.60	12.2%	

Table S3. SCLC charge mobility of the polymer:IT-4F blend films

Active layer	Ratio	μ_h[cm^2 V^{-1} s^{-1}]	μ_e [cm^2 V^{-1} s^{-1}]	μ_h/μ_e
F13:IT-4F	1:1.5	1.0×10^{-4}	2.0×10^{-5}	5.0
F13-R:IT-4F	1:1.5	6.5×10^{-5}	4.0×10^{-5}	1.6

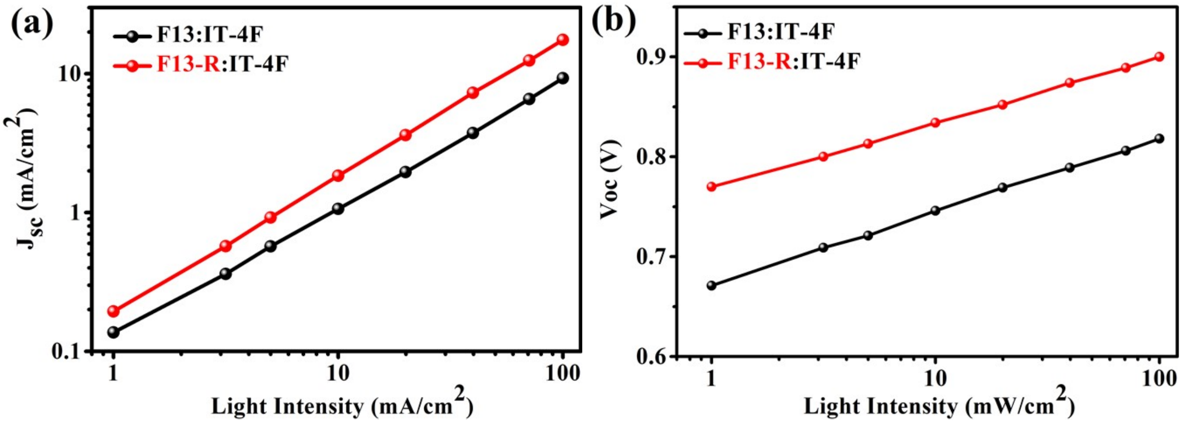

Fig. S3. (a) Light intensity dependence of J$_{sc}$ of as-cast PSCs based on F13:IT-4F and F13-R:IT-4F; (b) V$_{oc}$ versus light-intensity of as-cast PSCs based on F13:IT-4F and F13-R:IT-4F.

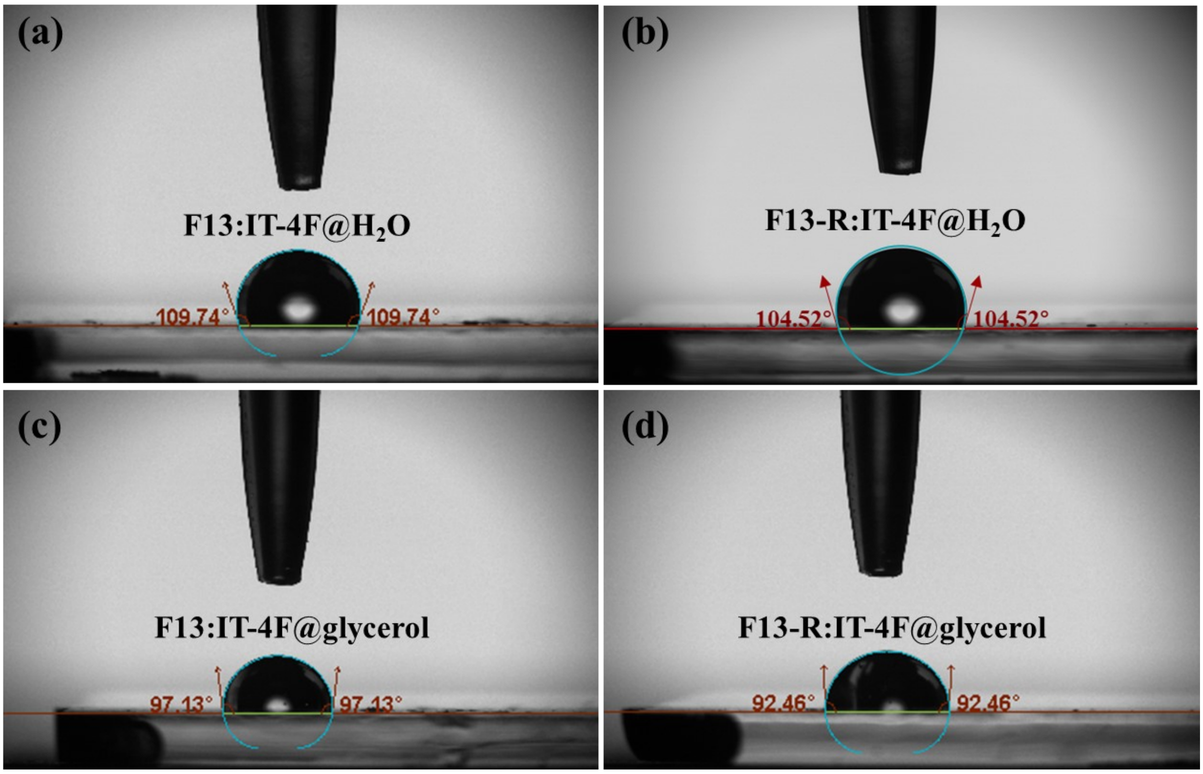

Fig. S4 The contact angles of water and glycerol on the surface of (a,c) F13:IT-4F blend film, (b,d)F13-R :IT-4F blend film.

References

1. S. C. Price, A. C. Stuart, L. Yang, H. Zhou and W. You, *J. Am. Chem. Soc.*, 2011, **133**, 8057-8057.
2. E. He, Z. Zheng, Y. Lu, F. Guo, S. Gao, X. Pang, G. T. Mola, L. Zhao and Y. Zhang, *J. Mater. Chem. A*, 2020, **8**, 11381-11390.
3. Y. Cui, H. Yao, L. Hong, T. Zhang, Y. Xu, K. Xian, B. Gao, J. Qin, J. Zhang, Z. Wei and J. Hou, *Adv. Mater.*, 2019, **31**, 1808356.
4. Y. Lin, Q. He, F. Zhao, L. Huo, J. Mai, X. Lu, C. J. Su, T. Li, J. Wang, J. Zhu, Y. Sun, C. Wang and X. Zhan, *J. Am. Chem. Soc.*, 2016, **138**, 2973-2976.
5. M. Zhao, Z. Qiao, X. Chen, C. Jiang, X. Li, Y. Li and H. Wang, *Polym. Chem.*, 2017, **8**, 5688-5697.
6. Q. Fan, Y. Wang, M. Zhang, B. Wu, X. Guo, Y. Jiang, W. Li, B. Guo, C. Ye, W. Su, J. Fang, X. Ou, F. Liu, Z. Wei, T. C. Sum, T. P. Russell and Y. Li, *Adv. Mater.*, 2018, **30**, 1704546.
7. Y. Yang, K. Wang, G. Li, X. Ran, X. Song, N. Gasparini, Q. Q. Zhang, X. Lai, X. Guo, F. Meng, M. Du, W. Huang and D. Baran, *Small*, 2018, **14**, 1801542.
8. X. Shi, X. Liao, K. Gao, L. Zuo, J. Chen, J. Zhao, F. Liu, Y. Chen and A. K. Y. Jen, *Adv. Funct. Mater.*, 2018, **28**, 1802324.
9. H. Huang, X. Li, L. Zhong, B. Qiu, Y. Yang, Z.-G. Zhang, Z. Zhang and Y. Li, *J. Mater. Chem. A*, 2018, **6**, 4670-4677.
10. Y. Liu, M. Li, J. Yang, W. Xue, S. Feng, J. Song, Z. Tang, W. Ma and Z. Bo, *Adv. Energy Mater.*, 2019, **9**, 1901280.
11. H. Feng, X. Song, Z. Zhang, R. Geng, J. Yu, L. Yang, D. Baran and W. Tang, *Adv. Funct. Mater.*, 2019, **29**, 1903269.
12. Q. He, M. Shahid, J. Wu, X. Jiao, F. D. Eisner, T. Hodsden, Z. Fei, T. D. Anthopoulos, C. R. McNeill, J. R. Durrant and M. Heeney, *Adv. Funct. Mater.*, 2019, **29**, 1904956.
13. T. Li, S. Dai, Z. Ke, L. Yang, J. Wang, C. Yan, W. Ma and X. Zhan, *Adv. Mater.*, 2018, **30**, 1705969.
14. P. Jiang, H. Lu, Q.-Q. Jia, S. Feng, C. Li, H.-B. Li and Z. Bo, *J. Mater. Chem. A*, 2019, **7**, 5943-5948.
15. B. Fan, D. Zhang, M. Li, W. Zhong, Z. Zeng, L. Ying, F. Huang and Y. Cao, *Sci. China Chem.*, 2019, **62**, 746-752.
16. F. Pan, L. Zhang, H. Jiang, D. Yuan, Y. Nian, Y. Cao and J. Chen, *J. Mater. Chem. A*, 2019, **7**, 9798-9806.
17. W. Su, Q. Fan, X. Guo, J. Wu, M. Zhang and Y. Li, *Phys. Chem. Chem. Phys.*, 2019, **21**, 10660-10666.
18. W. Liu, C. e. Zhang, J. Liu and Z. Bo, *ACS Appl. Mater. Inter.*, 2020, **12**, 37409-37417.
19. K. Wang, X. Song, X. Guo, Y. Wang, X. Lai, F. Meng, M. Du, D. Fan, R. Zhang, G. Li, A. K. K. Kyaw, J. Wang, W. Huang and D. Baran, *Mater. Chem. Front.*, 2020, **4**, 206-212.
20. J. Fang, Q. Liu, J. Zhang, L. Ye, J. Wu, Z. Wei, X. Guo, M. Zhang and Y. Li, *Solar RRL*, 2020, **4**, 2000275.
21. H. Jiang, G. Qin, L. Zhang, F. Pan, Z. Wu, Q. Wang, G. Wen, W. Zhang, Y. Cao and J. Chen, *J. Mater. Chem. C*, 2021, **9**, 249-259.

22. Z. Zhang, Y. Li, G. Cai, Y. Zhang, X. Lu and Y. Lin, *J. Am. Chem. Soc.*, 2020, **142**, 18741-18745.
23. M. Li, L. Yang, Y. Zhou, Y. Liu, J. Song, H. Wang and Z. Bo, *J. Phys. Chem. C*, 2021, **125**, 10841-10849.
24. N. Chandrasekaran, A. Kumar, L. Thomsen, D. Kabra and C. R. McNeill, *Mater. Adv.*, 2021, **2**, 2045-2054.
25. F. Du, H. Wang, Z. Zhang, L. Yang, J. Cao, J. Yu and W. Tang, *Mater. Horizons*, 2021, **8**, 1008-1016.